LETTERS

# Diapir-induced reorientation of Saturn's moon Enceladus

Francis Nimmo[1] & Robert T. Pappalardo[2]†

**Enceladus is a small icy satellite of Saturn. Its south polar region consists of young, tectonically deformed terrain and has an anomalously high heat flux[1,2]. This heat flux is probably due to localized tidal dissipation within either the ice shell[3] or the underlying silicate core[4]. The surface deformation is plausibly due to upwelling of low-density material (diapirism[5]) as a result of this tidal heating. Here we show that the current polar location of the hotspot can be explained by reorientation of the satellite's rotation axis because of the presence of a low-density diapir. If the diapir is in the ice shell, then the shell must be relatively thick and maintain significant rigidity (elastic thickness greater than ~0.5 km); if the diapir is in the silicate core, then Enceladus cannot possess a global subsurface ocean, because the core must be coupled to the overlying ice for reorientation to occur. The reorientation generates large (~10 MPa) tectonic stress patterns[6] that are compatible with the observed deformation of the south polar region[2]. We predict that the distribution of impact craters on the surface will not show the usual leading hemisphere–trailing hemisphere asymmetry. A low-density diapir also yields a potentially observable negative gravity anomaly.**

Enceladus (radius 252 km) is near the 2:1 mean motion resonance with Dione, forcing its orbital eccentricity to 0.0047. Tidal heating[3,7], possibly including either resonant libration[8] or interactions with the satellite Janus[9], is probably sufficient to cause geological activity; the maximum likely heat output is of the order of $10^3$ GW (ref. 3). This tidal deformation may also lead to localized shear heating[2,10] along active polar tectonic features observed by the Cassini spacecraft.

The ~300-km-wide, tectonically deformed southern region of Enceladus[2], and other older deformed regions, show some resemblance to the three tectonically deformed 'coronae' on the similarly small (236 km radius) uranian satellite Miranda[5,11]. Miranda's coronae are analogously ovoidal and large (~200–300 km across), are tectonically deformed with distinct inner and outer deformation zones, and are located along the satellite's larger principal axes of inertia. They are generally inferred to be regions of tectonic deformation and icy volcanism above large-scale ice diapirs[5,11]. The location of the coronae suggests that true polar wander occurred[12], and past reorientation is consistent with spatial variations in the distribution of fresh craters on Miranda[13]. On Earth and Mars, convective upwellings are likely to have resulted in true polar wander in the past[14,15], while ice shell thickness variations may have caused similar effects on Jupiter's moon Europa[16].

Tidal heating within the silicate core of Enceladus[4] may produce warm silicate upwellings there, and could also lead to diapirism in a sufficiently thick overlying ice shell. Alternatively, localized heating within the ice shell itself may cause a low-density diapir[17]. Below, we consider the circumstances under which a large, low-density diapir in either the silicate or the ice portion of Enceladus could have caused reorientation of the satellite, moving the diapiric region towards the satellite's spin axis.

We first consider an ice diapir, as depicted in Fig. 1. If the overlying lithosphere has negligible rigidity, the mass deficit at depth will be compensated by a surface mass excess, generated by upwarped topography. Because that mass excess is closer to the surface than the interior mass deficit, the net effect is to generate a positive gravitational potential anomaly, which would tend to reorient the region towards the equator. In contrast, for the case of an infinitely rigid lithosphere, there would be no surface topography, thus producing a net negative potential anomaly, tending to reorient the region towards the pole. A subsurface diapir therefore can result in either poleward or equatorward reorientation, depending on the rigidity (or elastic thickness) of the lithosphere[16]. Reorientation is opposed by the frozen-in component of the triaxial satellite's tidal and rotational bulges[18,19]; thus, other things being equal, a satellite with lower rigidity will have smaller permanent bulges and is more likely to undergo reorientation.

Reorientation is favoured if density anomalies persist for times long compared to the viscous relaxation timescale[18,20]. This condition

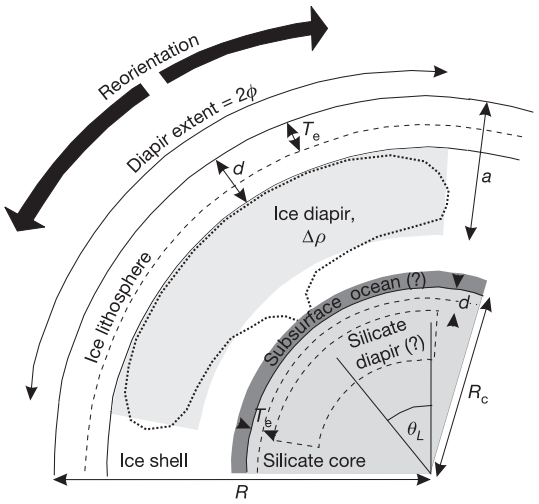


**Figure 1 | Schematic diagram of subsurface diapirism on Enceladus.** The light shaded area approximates the shape of an inferred diapir (dotted line) in the ice shell, and has a density contrast $\Delta\rho$ with the surrounding ice. The dashed region within the darker shaded area denotes an alternative diapir location within the silicate core. For ice and silicate densities of 950 kg m$^{-3}$ and 3,500 kg m$^{-3}$, respectively, $R_c = 161$ km using a bulk density for Enceladus[2] of 1,610 kg m$^{-3}$. For the ice diapir we use $a = 91$ km; for the silicate diapir $a = 155$ km, and $d$ and $T_e$ are measured from the surface of the silicate core. In both cases, $\phi = 35°$ and the initial load colatitude $\theta_L = 45°$.

[1]Department of Earth Sciences, University of California Santa Cruz, 1156 High Street, Santa Cruz, California 95064, USA. [2]Laboratory for Atmospheric and Space Physics, University of Colorado, Boulder, Colorado 80309-0392, USA. †Present address: Earth and Space Sciences Division, Jet Propulsion Laboratory, Pasadena, California 91109, USA.

is likely to be satisfied on Enceladus for both the ice shell[16] and silicate core[14]. Following the approach of Matsuyama *et al.*[18], for a synchronously rotating satellite, the long-term angular reorientation $\delta$ due to an imposed potential anomaly is given by

$$\delta = \frac{1}{2}\tan^{-1}\left(\frac{Q^{\star}\sin 2\theta_L}{n - Q^{\star}\cos 2\theta_L}\right) \quad (1)$$

where $\theta_L$ is the initial colatitude of the centre of the anomaly, $n$ is a parameter that depends on the longitudinal location of the anomaly relative to the tidal bulge (see Supplementary Information), and $Q^{\star}$ is a parameter that describes both the size of the potential anomaly and the non-hydrostatic component of rotational flattening, which opposes reorientation.

The quantity $Q^{\star}$ is given[18] by $Q^{\star} = 3\sqrt{5}G_{20}/R^2\Omega^2(k_2^f - k_2)$where $G_{20}$ is the second-degree potential anomaly due to the diapir, $R$ is the mean satellite radius, $\Omega$ is the rotation angular frequency of the satellite, and $k_2^f$ and $k_2$ are the degree-two tidal Love numbers for the satellite without and with an elastic layer, respectively[18]. Smaller values of $k_2$ result in a larger permanent bulge and less reorientation, while larger potential anomalies result in greater reorientation. Here we calculate $k_2$ using a multi-layered Maxwell viscoelastic model[21] in which all regions except the elastic part of the lithosphere are assumed to be inviscid (Supplementary Information).

The second-degree potential anomaly $G_{20}$ due to a partially compensated load depends on the diapir angular half-width $\phi$ and radial extent $a - d$ (see Fig. 1), the density contrast between the diapir and the surrounding material $\Delta\rho$, and the degree of compensation $C$, and is derived in the Supplementary Information. $C$ depends on the ability of the cold elastic part of the ice or silicate layer (thickness $T_e$; see Fig. 1) to resist deformation, and is calculated using the method of ref. 22.

Figure 2a shows how $Q^{\star}$, $C$ and $k_2$ vary as a function of lithospheric thickness $d$, where, following ref. 23, the elastic thickness $T_e = 0.4d$ above either silicate or ice diapirs. For the ice diapir (solid lines), the degree of compensation $C$ decreases as $d$ increases. At some critical degree of compensation (~0.8 in this case) the potential anomaly switches from positive to negative, and as a result so does $Q^{\star}$. This indicates that at greater elastic thicknesses, the diapir will reorient towards the pole. The solid lines in Fig. 2b show the angular reorientation (equation (1)) produced by an ice diapir. Lower load latitudes generally lead to greater reorientation, and larger density contrasts lead to greater reorientation. Low values of $d$ lead to equatorward motion, while $d$ values in excess of ~1.3 km lead to poleward reorientation.

The solid curves in Fig. 2 demonstrate that an ice diapir within a thick shell and with a sufficiently large density contrast can lead to significant poleward reorientation (up to 30°), if the elastic thickness exceeds ~0.5 km. Thus, if an ice diapir has reoriented Enceladus, the polar location of the active region suggests that the satellite has retained some near-surface rigidity, despite the observed surface deformation. An elastic thickness of ~0.5 km is similar to results obtained for Ganymede[23], which apparently underwent an ancient episode of tidal deformation and heating. Similarly, the elastic thickness of Miranda in regions adjacent to the coronae was ~2 km at the time of deformation[5].

Figure 2 also shows that large density contrasts are required to achieve significant reorientation, suggesting that an ice diapir must be primarily compositional, rather than thermal, in origin. Partial melting of a tidally heated diapir will preferentially remove low-melting-temperature, dense components, such as salts, leading to compositional buoyancy[17,24].

The reorientation due to a diapir within the silicate core (dashed lines in Fig. 2) is comparable to that for an ice diapir, and promotes poleward reorientation. A co-axial combination of silicate and ice diapirism would lead to larger angular reorientations, because the reorientation depends on the total potential anomaly.

Observations of the tectonic deformation around the south pole of Enceladus[2] support the reorientation hypothesis. The observed orientations of polar contractional and lower-latitude extensional structures are consistent with the stress patterns generated by moderate true polar wander[6]. Strike-slip activity in subpolar latitudes is also predicted, and will provide an additional observational test of the hypothesis. If the flattening of Enceladus is close to hydrostatic[2], a 30° reorientation will give rise to stresses approaching 10 MPa (ref. 6), easily enough to generate significant deformation.

We can think of at least two additional tests. First, the distribution of impact craters—expected to show leading–trailing hemisphere asymmetry if the satellite orbits synchronously—will be affected by, and could constrain, reorientation[13]. Second, Fig. 2 shows that a negative, long-wavelength gravity anomaly (with an amplitude of a few mGal at 200 km spacecraft altitude) will be associated with the anomalous south polar region. Regional gravity anomalies similar to this have been detected at Ganymede by the Galileo spacecraft[25].

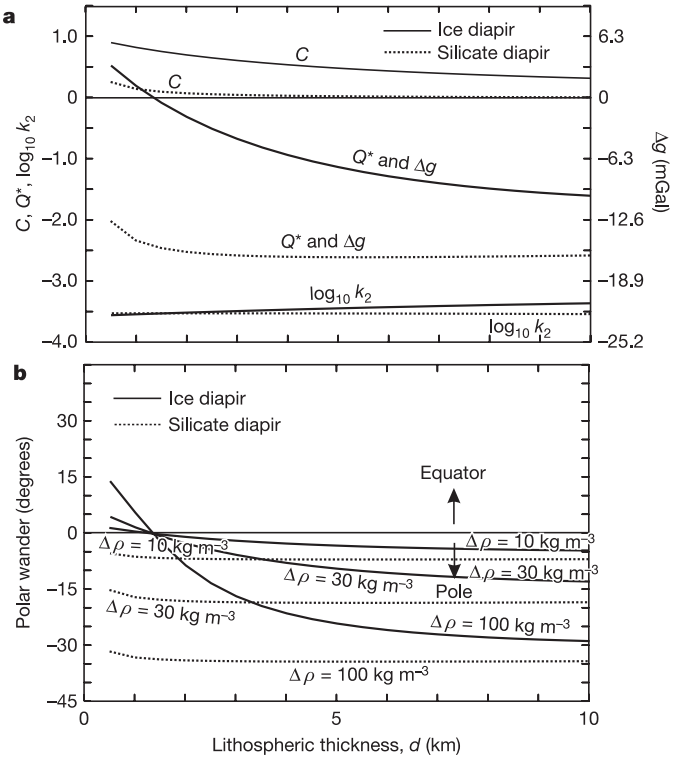


**Figure 2 | Variation of parameters affecting reorientation, and the degree of reorientation itself, as a function of *d*, the lithospheric thickness. a**, $C$ is the compensation factor, $Q^{\star}$ is the reorientation factor defined in the text, and $k_2$ is the Love number. Love numbers are calculated using a multi-layer Maxwell viscoelastic code[21] (see Supplementary Information). Other parameters are defined in Fig. 1 legend. The elastic thickness $T_e = 0.4d$, the fluid Love number $k_2^f = 0.75$ and the satellite rotation frequency $\Omega = 5.31 \times 10^{-5}\,s^{-1}$. Solid lines denote ice diapir; dashed lines denote silicate diapir. For the ice diapir case the silicate core is assumed to behave elastically, resulting in a reduced $k_2$. Importantly, because $k_2 \ll k_2^f$ the denominator of $Q^{\star}$ is almost independent of $k_2$ and thus neither $Q^{\star}$ nor the amount of reorientation are very sensitive to the value of $k_2$ adopted. The quantity $\Delta g$ is the degree-2 gravity anomaly in mGal (right-hand scale), which is proportional to $Q^{\star}$ and is derived by assuming a spacecraft altitude of 200 km (see Supplementary Information). $Q^{\star}$ and $\Delta g$ are calculated using $\Delta\rho = 100\,kg\,m^{-3}$. **b**, Angular reorientation $\delta$ (equation (1)) as a function of $d$ for different density contrasts. Positive values of $\delta$ indicate equatorward reorientation; negative values indicate poleward reorientation. We use $\theta_L = 45°$, $\phi = 35°$, $n = 1$. The reorientation for a silicate diapir is much less sensitive to the elastic thickness assumed than that for an ice diapir, because the higher rigidity of silicates compared to ices means that the compensation factor $C$ is close to zero for the range of $T_e$ values that we considered (Fig. 2a).

We can also test whether the inferred reorientation is due to diapirism within the ice shell, the silicate core, or indeed some combination of the two. First, reorientation due to an ice diapir requires an elastic thickness in excess of ~0.5 km. This requirement can be compared with $T_e$ values inferred using local topographic measurements[23]. Second, if diapirism in the silicate core is primarily responsible for the inferred reorientation, the ice shell must be efficiently coupled to the rocky core beneath. The effect of a global subsurface ocean would be to decouple the shell from the underlying material[16]; thus, if a silicate diapir is responsible for reorientation, Enceladus must lack a global subsurface ocean. Subsurface oceans have been detected in several galilean satellites, but detecting an internal ocean using magnetometry in the Saturn system is significantly more challenging.

There are several additional effects that we have not included. We have neglected both the inhibiting effect of dissipation caused by the reorientation itself[16], and possible spatial variations in $T_e$. Enceladus' orbital eccentricity, and thus the amount of tidal heating, is unlikely to have been constant through time[26]. This raises the possibility that more than one diapir may have arisen, leading to successive reorientations of the body and a complicated (but potentially decipherable) deformation history. Similarly, the dimensions and density contrast of each rising diapir, and the elastic thickness of the overlying rigid layer, are likely to have changed with time, generating more complicated and potentially non-monotonic reorientation paths[14,15,18,20]. However, our main conclusions are unlikely to be affected by these details.

The principal requirements for reorientation to occur are the development of sufficiently large and long-lived density contrasts of sufficient lateral and radial extent. Unless there are large vertical viscosity gradients[27], vigorous convection is unlikely to generate such contrasts, because both the characteristic length scales and timescales of convective features tend to be small at high Rayleigh numbers[14]. Conversely, the initiation of either convection or a Rayleigh–Taylor upwelling will occur on a length scale that is usually comparable to the fluid layer depth[28]. Thus, bodies which are, or once were, active enough to generate density contrasts, but not to convect vigorously, are most likely to have undergone reorientation. The mid-sized icy satellites, including those of Saturn, have in many cases undergone geological deformation in the past[29], and are expected to be close to the onset of convection[30]. We therefore anticipate possible additional examples of mid-sized satellite reorientation as more Cassini data are returned.

**Received 15 March; accepted 10 April 2006.**


1. Spencer, J. R. *et al.* Cassini encounters Enceladus: Background and the discovery of a south polar hot spot. *Science* **311,** 1401–1405 (2006).
2. Porco, C. C. *et al.* Cassini observes the active south pole of Enceladus. *Science* **311,** 1393–1401 (2006).
3. Ross, M. N. & Schubert, G. Viscoelastic models of tidal heating in Enceladus. *Icarus* **78,** 90–101 (1989).
4. Matson, D. L. *et al.* Enceladus' interior and geysers–possibility for hydrothermal geochemistry. *Lunar Planet Sci. Conf.* **XXXVII,** abstr. 2219 (2006).
5. Pappalardo, R. T., Reynolds, S. J. & Greeley, R. Extensional tilt blocks on Miranda: Evidence for an upwelling origin of Arden Corona. *J. Geophys. Res.* **102,** 13369–13379 (1997).
6. Melosh, H. J. Tectonic patterns on a reoriented planet: Mars. *Icarus* **44,** 745–751 (1980).
7. Squyres, S. W., Reynolds, R. T. & Cassen, P. M. The evolution of Enceladus. *Icarus* **53,** 319–331 (1983).
8. Wisdom, J. Spin-orbit secondary resonance dynamics of Enceladus. *Astron. J.* **128,** 484–491 (2004).
9. Lissauer, J. J., Peale, S. J. & Cuzzi, J. N. Ring torque on Janus and the melting of Enceladus. *Icarus* **58,** 159–168 (1984).
10. Gaidos, E. & Nimmo, F. Tectonics and water on Europa. *Nature* **405,** 637 (2000).
11. Greenberg, R., *et al.* in *Uranus* (eds Bergstralh, J. T. *et al.*) 693–735 (Univ. Arizona Press, Tucson, 1991).
12. Janes, D. M. & Melosh, H. J. Sinker tectonics–an approach to the surface of Miranda. *J. Geophys. Res.* **93,** 3127–3143 (1988).
13. Plescia, J. B. Cratering history of Miranda–implications for geologic processes. *Icarus* **73,** 442–461 (1988).
14. Richards, M. A., Bunge, H. P., Ricard, Y. & Baumgardner, J. R. Polar wandering in mantle convection models. *Geophys. Res. Lett.* **26,** 1777–1780 (1999).
15. Moser, J., Yuen, D. A., Larsen, T. B. & Matyska, C. Dynamical influences of depth-dependent properties on mantle upwellings and temporal variations of the moment of inertia. *Phys. Earth Planet. Inter.* **102,** 153–170 (1997).
16. Ojakangas, G. W. & Stevenson, D. J. Polar wander of an ice shell on Europa. *Icarus* **81,** 242–270 (1989).
17. Sotin, C., Head, J. W. & Tobie, G. Europa: tidal heating of upwelling thermal plumes and the origin of lenticulae and chaos melting. *Geophys. Res. Lett.* **29,** 1233, doi:10.1029/2001GL013844 (2002).
18. Matsuyama, I., Mitrovica, J. X., Manga, M., Perron, J. T. & Richards, M. A. Rotational stability of dynamic planets with elastic lithospheres. *J. Geophys. Res.* **111,** E02003, doi:10.1029/2005JE002447 (2006).
19. Willemann, R. J. Reorientation of planets with elastic lithospheres. *Icarus* **60,** 701–709 (1984).
20. Tsai, V. C. & Stevenson, D. J. Theoretical constraints on true polar wander. *Eos* **86,** GP21A–02 (2005).
21. Moore, W. B. & Schubert, G. The tidal response of Europa. *Icarus* **147,** 317–319 (2000).
22. Turcotte, D. L., Willemann, R. J., Haxby, W. F. & Norberry, J. Role of membrane stresses in the support of planetary topography. *J. Geophys. Res.* **86,** 3951–3959 (1981).
23. Nimmo, F., Pappalardo, R. T. & Giese, B. Elastic thickness and heat flux estimates on Ganymede. *Geophys. Res. Lett.* **29,** doi:10.1029/2001GL013976 (2002).
24. Nimmo, F., Pappalardo, R. T. & Giese, B. On the origins of band topography Europa. *Icarus* **166,** 21–32 (2003).
25. Palguta, J., Anderson, J. D., Schubert, G. & Moore, W. B. Mass anomalies on Ganymede. *Icarus* **180,** 428–441 (2006).
26. Ojakangas, G. W. & Stevenson, D. J. Episodic volcanism of tidally-heated satellites with application to Io. *Icarus* **66,** 341–358 (1986).
27. McNamara, A. K. & Zhong, S. J. Degree-one mantle convection: Dependence on internal heating and temperature-dependent rheology. *Geophys. Res. Lett.* **32,** L01301, doi:10.1029/2004GL021082 (2005).
28. Turcotte, D. L. & Schubert, G. *Geodynamics* 2nd edn (Cambridge Univ. Press, Cambridge, UK, 2002).
29. Morrison, D., Owen, T. & Soderblom, L. A. in *Satellites* (eds Burns, J. A. & Matthews, M. S.) 764–801 (Univ. Arizona Press, Tucson, 1986).
30. McKinnon, W. B. in *Solar System Ices* (eds Schmitt, B., de Bergh, C. & Festou, M.) 525–550 (Kluwer Academic, Dordrecht, 1998).


**Supplementary Information** is linked to the online version of the paper at www.nature.com/nature.

**Acknowledgements** We thank J. Moore, J. Melosh and M. Mullen for comments. This research was supported by NASA PGG and OPR.

**Author Information** Reprints and permissions information is available at npg.nature.com/reprintsandpermissions. The authors declare no competing financial interests. Correspondence and requests for materials should be addressed to F.N. (fnimmo@es.ucsc.edu).